Memory Effects in Gel–Solid Transformations: Coordinately Unsaturated Al Sites in Nanosized Aluminas

Dominique Coster and Jose J. Fripiat*

Department of Chemistry and Laboratory for Surface Studies, University of Wisconsin—Milwaukee, P.O. Box 413, Milwaukee, Wisconsin 53201

Received February 19, 1993. Revised Manuscript Received May 4, 1993

Precursors of aluminas rich in pentacoordinated aluminum are generated by a new sol–gel route. The critical step of the process is a limited hydrolysis of aluminum *tri.sec.*butoxide in non-aqueous media. The gel–solid transformation is investigated by ^{27}Al high-resolution MAS NMR and nitrogen adsorption. The structural and textural evolutions of the gel by thermal activation up to 700 °C are self-determined. As the octahedral condensation in the gel increases, the Al^{V} concentration in the solid increases: this observation evidences a structural memory. The percentage of small pores ($d < 6$ nm) in the transition alumina is correlated to the chemical shift of the Al^{VI} line in the gel. Thus, a textural memory effect is also observed. A general mechanism for the Al^{V} formation is proposed, and the metastability of this coordinately unsaturated aluminum site is demonstrated.

Introduction

The ^{27}Al high-resolution nuclear magnetic resonance of finely ground gibbsite[1] or boehmite[2] shows the following characteristics. Beside the main peak corresponding to 6-fold coordinated aluminum (Al^{VI}) a contribution assigned to pentacoordinated species (Al^{V}) is also observed as well as a weak signal attributable to 4-fold coordinated aluminum (Al^{IV}). In the unground precursor, the only observable species is Al^{VI}. Mechanical grinding increases the specific area of boehmite from 9 to 130 m^2g^{-1}. After calcining the unground precursor to 600 °C a transition (X-ray amorphous) alumina is obtained in which the relative Al^{IV} content is about 50% of the relative Al^{VI} content, as expected in a pseudo-spinel structure. During this process, and because of dehydroxylation, the surface area is multiplied by a factor of ~10 but no bulk Al^{V} is detectable. On the contrary, calcining the ground boehmite to 600 °C somewhat increases the Al^{IV} content, and the ratio Al^{IV}:Al^{V}:Al^{VI} is 1:1:2. The specific surface area remains about the same (~100 m^2 g^{-1}). Thus, grinding introduces coordinately unsaturated Al^{V} sites (CUS) while thermal activation does not. In spite of the important structure reconstruction provoked by dehydroxylation, the calcined solid keeps the memory of the structural defects created by the mechanical action.

Recently, Wood *et al.*[3] have published a procedure for obtaining solids rich in Al^{V} based on the solution chemistry of aluminum. The gels giving successful results, in terms of the relative abundance in Al^{V}, were obtained by a two-step technique. The hydrolysis of either $AlCl_3$ or $Al(NO_3)_3$ was carried out in aqueous solution using 2.5 equiv of either urea or hexamethylenetetramine per aluminum and the mixture is aged at 90 °C for 3 days. Afterward, 0.5 equiv of ammonium bicarbonate is added, and the gel is immediately washed by centrifugation and dried at 85 °C. Thermal activation above 300 °C gives a solid rich in Al^{V}. This detailed procedure is reported because it has inspired our work.

As widely recognized, the solution chemistry of aluminum is very complex, and Wood *et al.*[3] give an excellent review of the diversity of aluminum cation speciation. However, the role of their different additives is not clear. Most probably, the bicarbonate provokes the flocculation, but the action of urea is difficult to visualize. In 1933 Bunn[4] observed that the growth of NH_4Cl crystals is very different in the presence or absence of urea. One molecule of urea to twelve molecules of NH_4Cl is sufficient to inhibit the growth in the axial direction. The reason is a strong adsorption of urea on the corresponding plane.

The lesson of this early observation is that urea seems to be an inhibitor of crystal growth. Thus, the urea might restrict the condensation of octahedral units in the alumina gel precursor, or it may complex the Al oligomers, as suggested by Wood *et al.*[3] The ^{27}Al NMR spectrum of the Al^{3+} solution hydrolyzed in the presence of urea published by these authors shows a very broad line extending from −100 to +100 ppm, from which emerges a sharp Al^{IV} resonance line at about 60 ppm, while in the corresponding gel (dried at 85 °C) broad Al^{VI} and Al^{IV} lines are observed. A high background in the 30–40 ppm region may prevent the observation of the Al^{V} line. The latter is distinctly observed after thermal activation of the gel at, and above, 200 °C. The high relative concentration of Al^{V} in these solids is assigned by Wood *et al.* to the creation of oxygen vacancies driven by the movement of aluminum from octahedral to tetrahedral sites. Thus, the suggested mechanism is essentially thermal. Alternately, it might be that urea replaces oxygen octahedral ligands leaving CUS after thermal activation. Thus, the mechanical grinding of aluminum hydroxides and the aqueous hydrolysis of aluminum salts in the presence of urea generate precursors containing Al^{V}.

To gain information on these aluminas rich in Al^{V}, we have chosen another approach of preparation based on a

(1) Paramzin, J. M.; Zolotovskii, B. P.; Krivoruchko, O. P.; Buyanov, R. A. *Proc. VI Intern. Symp. Heterogeneous Catal. Sofia, Part 2* **1987**, 369.
(2) Chen, J. R.; Davis; J. G.; Fripiat, J. J. *J. Catal.* **1992**, *133*, 263.
(3) Wood, T. E.; Siedle, A. R.; Hill, J. R.; Skarjune, R. P.; Goodbrake, C. J. *Mater. Res. Symp. V110* **1990**, 97.
(4) Bunn, C. W. *Proc. R. Soc. London A* **1933**, *141*, 567.

0897-4756/93/2805-1204$04.00/0

sol–gel process in nonaqueous solvents. There have been numerous studies on the molecular structure of aluminum alkoxides. Among the recent ones, Kriz *et al.*[5] have shown the existence in benzene solution of Al alkoxides polymers with Al in 4-, 5-, and 6-fold coordination. From a detailed analysis of 13 different alkoxides, dimeric (2 Al^{VI}), trimeric (2 Al^{IV} + 1 Al^{VI}), cyclic (4 Al^{IV}), and tricyclic (Al^{VI} + 3 Al^{IV}) polymeric species have been identified.

Surprisingly, the limited hydrolysis of Al–alkoxide in nonaqueous solvents has drawn almost no attention up to now. Our basic idea has been to induce a very restricted hydrolysis in order to produce larger polymeric species. Then, the sol is transformed rapidly into a gel by flocculation. The calcination eliminates the organic residues and generates a solid rich in coordinatively unsaturated Al^{V} sites. The mechanisms of sol–gel transformation have been reviewed by Brinker and Scherer,[6] but mostly in aqueous conditions. For instance, in the Yoldas process aluminum tri-*sec*-butoxide is hydrolyzed in acidic conditions leading to a fibrillar boehmite.

In restricting the amount of water it was hoped that the sol and gel, obtained after the flocculation, would keep structural features such as Al^{IV} and Al^{V}. By contrast, in acidic aqueous conditions the aluminum gel contains Al^{VI} only as the result of hydrolysis and alcoxolation.[6]

This contribution will demonstrate that the early development of the sol determines almost completely its evolution into the gel and into the calcined solid. Even a thermal treatment (up to 700 °C) cannot erase the gel memory in spite of a complete removal of carbon.

Experimental Section

Materials. A 0.4 M Al tri-*sec*-butoxide in *sec*-butanol solution was added to an urea solution in *sec*-butanol so that the urea/Al molar ratio was 4/3. Water was added to that mixture in order to achieve a molar ratio $H_2O/Al \simeq 0.7$. In a variant procedure glacial acetic acid was used in order to yield the same H_2O/Al ratio. In that case, the water being produced by *in situ* esterification of the acid by the alcohol is more homogeneously distributed in the reacting mixture.

Whatever the nature of the mixture, the sol was aged at 85 °C for 3 days upon stirring. During that period of time partial hydrolysis of the butoxide occurred. After the aging period ammonium bicarbonate was added at room temperature (molar ratio bicarbonate/Al $\simeq$ 0.5) under stirring in order to precipitate the gel. If ammonium bicarbonate is not used, the yield in gel was very low, most of the sol being washed out.

The gel was thoroughly washed by centrifugation with *sec*-butanol in order to get rid of the unreacted Al tri-*sec*-butoxide. Thereafter, it was freeze dried and then dried between 70 and 85 °C for 12 h to remove the solvent and stored over P_2O_5. Unless otherwise noted, the standard calcination procedure used to produced the solid consisted in increasing the temperature at 150 °C/h to 550 °C, and in keeping this temperature constant for 20 h. The solid was stored over P_2O_5.

The gel and solid are characterized by three digits referring to the gel preparation. The first, second, and third digits correspond to the addition of urea, ammonium bicarbonate, and water, respectively. The code is eventually followed by symbols referring to some particular aspects of the procedure which will be commented on. For instance, the solid 012 is obtained after standard calcination of the 012 gel. The latter has been prepared without urea, the regular amount of NH_4HCO_3 has been used, while the water content is the double of the standard procedure. The symbol Ac refers to the gel prepared using the acetic acid esterification (for instance, 00Ac means no urea, no ammonium bicarbonate). Eleven gels and solids were characterized as described in the next paragraph.

Characterization Techniques. The gels were characterized by differential thermal (DTA) or thermogravimetric (TGA) analysis, the rate of the temperature increase being 10 °C/min. Weight losses were also measured separately between 85 and 1000 °C. The ^{27}Al nuclear magnetic resonance spectra of the gels and of the solids were obtained under the following conditions: magic angle spinning (MAS) ~12 kHz; Larmor frequency 130.3 MHz; pulse lengths 0.5 μs; delay between pulses 50 ms; number of accumulations: between 2 and 4 × 10^3. Other experiments such as nutation and proton–aluminum cross-polarization will be reported elsewhere.

The complete N_2 adsorption–desorption isotherms were measured on solids outgassed at 300 °C for 2 h before the run, using the Omnisorb 100 (Coulter Co.) in the static mode. The pore-size distribution was measured using the technique of Barret *et al.*[7] Carbon and nitrogen analyses were carried out on six gels. The results were interpreted as follows: The nitrogen content was assigned to either residual urea or ammonium bicarbonate. The carbon content, minus that in urea or bicarbonate, was attributed to residual Al *sec*-butoxyl linkages, still present in the gel because of the restricted hydrolysis. The difference between the total weight loss and the sum (*sec*-butoxyls + urea or NH_4HCO_3) was considered as the amount of water retained in the gel. These calculations must be considered as approximate, because the retention of the solvent is neglected. Note that there was no nitrogen left in the solids and that their carbon content was less than 0.3%.

A typical 111 gel was examined by transmission electron microscopy at high resolution. Also, X-ray (Cu Kα) diffractograms were recorded in a high-temperature chamber in which a 111 gel was heated at 100, 300, 500, 650, 750, 900, and 1100 °C for 1 h. A broad and weak reflection was observed at d = 3.5 Å from 100 to 900 °C. This result will not be commented on further, since the solids are X-ray amorphous. Note, however, that on heating to 1100 °C the reflections typical of α-Al_2O_3 were observed. No reflection attributable to ammonium bicarbonate was observed after treatment at 100 °C.

Results

Gels. The gels have been characterized by TEM, ^{27}Al MAS NMR, as well as by chemical analyses. It should be emphasized that these characterizations were performed after the gels have been dried in the temperature range 70–85 °C in the air and that during drying it is likely that some additional hydrolysis occurred. Moreover, a fraction of the residual urea and/or NH_4HCO_3 have been driven out.

The morphological features of a typical 111 gel are shown in Figure 1. Small particles, with diameters smaller than 300 Å, are entangled in fluffy large and porous aggregates. The electron diffraction of aggregates reveals two faint and broad halos corresponding to d spacings of $\simeq$2.00 and 1.15 Å. Some spots are observed occasionally, but they never form an interpretable pattern.

The results of the chemical analysis and weight losses are listed in Table I. It includes the molar ratios H_2O/Al *sec*-butoxy/Al, and the number of (OH plus *sec*-butoxyls) ligands per Al. The number of Al–O–Al ligands is, of course, not computable. The results in Table I do not show a clear relationship between the sol preparation and the molar ratios.

The deconvolution and the characteristic of the ^{27}Al MAS NMR spectra of the gels are shown in Table II while Figure 2a gives an example of the ^{27}Al spectrum. The 4-,

(5) Kriz, O.; Casensky, B.; Lycka, A.; Fusek, J.; Hermanek, S. *J. Magn. Reson.* **1984**, *60*, 375.

(6) Brinker, C. J.; Scherer, G. W. *Sol-Gel Science*; Academic Press: New York, 1990.

(7) Barret, E. P.; Joyner, L. G.; Halenda, P. H. *J. Am. Chem. Soc.* **1951**, *73*, 373.

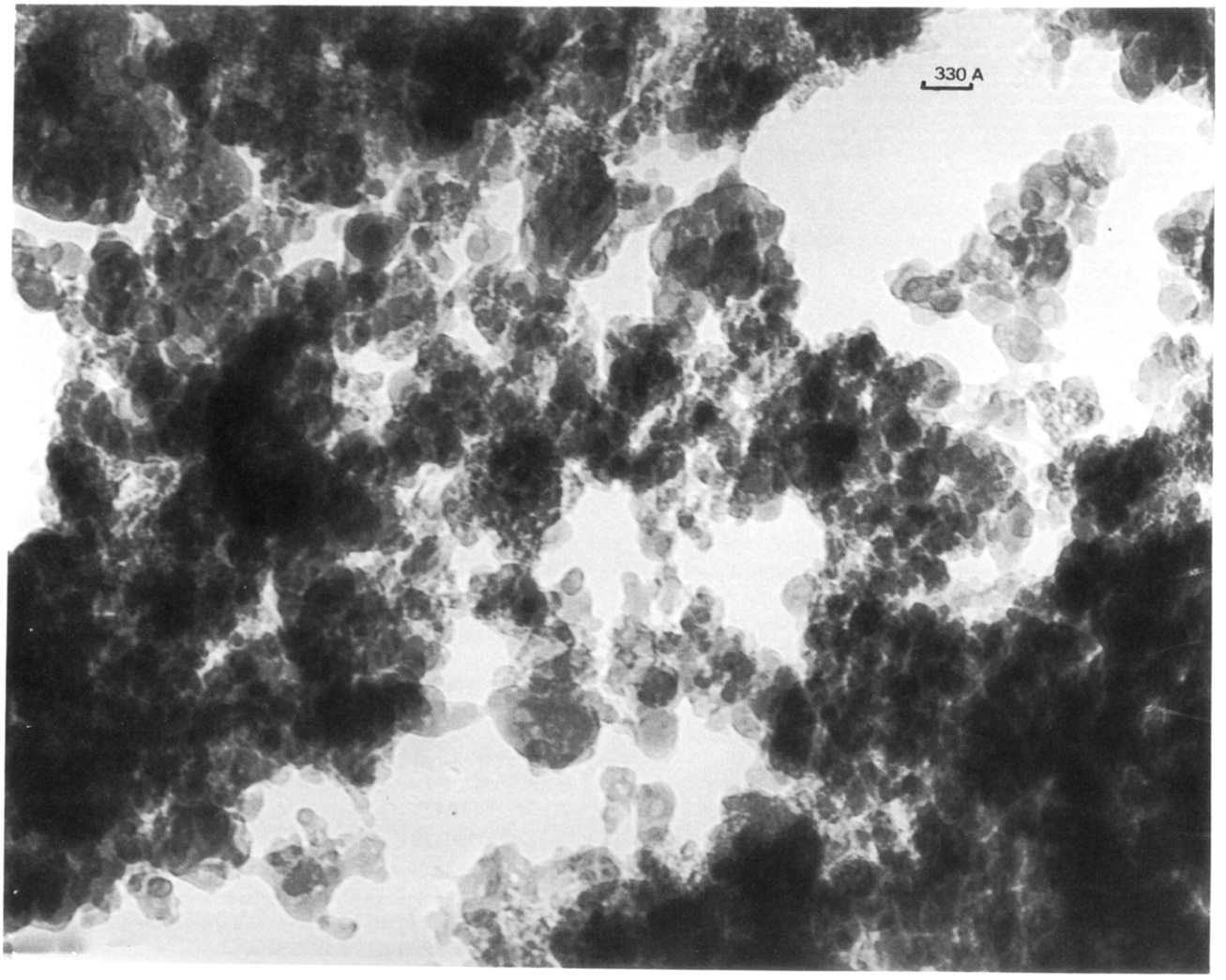

Figure 1. High-resolution transmission electronmicrograph of the 111 gel.

Table I. Results of the Chemical Analysis of the Gels Expressed as Molar Ratios H_2O/Al, *sec*-Butoxyl/Al: Number of Ligands per Al (ligd/Al) Is ($2H_2O$/Al + *sec*-but/Al)

code	H_2O/Al	*sec*-but/Al	ligd/Al
111 A[a]	0.558	0.154	1.272
011	0.478	0.299	1.255
001	0.659	0.150	1.468
101	0.649	0.523	1.923
111 NFD[b]	1.010	0.329	2.349
112	0.860	0.804	2.524

[a] Symbol A is used to differentiate from other 111 gels. [b] NFD means not freeze-dried.

Table II. ^{27}Al MAS NMR Results Obtained for the Gel

code	Al^{VI} shift (ppm)	% Al^{IV}	% Al^{V}	% Al^{VI}
111nW2[a]	3.55	30.4	38	31.6
111A	4.37	24.2	27.4	48.4
111	4.67	24.6	22.8	52.6
011	5.45	21.8	23.6	54.6
111W2[b]	5.48	21.4	25	53.6
001	6.0	21.4	25	53.6
101	6.95	20	13.3	66.7
111NFD	7.22	10.7	9.7	79.6
112	7.7	13.5	13.5	73.0
012	7.9	12.2	4.0	83.8
00Ac	4.4	~0	6.6	93.4

[a] nW2 is a gel in which the excess alkoxide has not been washed before freeze drying and drying. [b] W2 is a symbol used to distinguish a 111 gel preparation from others, as is symbol A.

5-, and 6-fold coordinated Al (Al^{IV}, Al^{V}, and Al^{VI}) resonance lines are well separated.

The first striking observation in Table II is the increase of the Al^{VI} contribution as the Al^{VI} line is shifted downfield. It is known that this line shifts downfield as the degree of polymerization, or of condensation, of the Al octahedra increases.[8] Thus, the increase in Al^{VI} content corresponds to an increase in the degree of polymerization of the octahedra. Reciprocally, the gels with a lower degree of polymerization have a larger contribution of Al^{V} and Al^{VI}. In Table II the only exception to the rule is the 00Ac gel which has the highest Al^{VI} content, while the Al^{VI} line has a large upfield shift. This may be due to the blockage of the polymerization by the formation of Al–O–Ac. It is also observed that increasing the amount of liquid water in the sol precursor (see gels 112 and 012, for instance) or skipping the freeze-drying step produce gels with higher Al^{VI} condensation.

Another interesting observation is reported in Figure 3. Here, the relative Al^{VI} intensity is shown with respect to the average number of OH plus *sec*-butoxyl ligands per Al (Table I). The larger this number, the larger is the Al^{VI} contribution and the higher the shift of the Al^{VI} line.

2. Solids. A. Structural Aspects. The solids obtained after calcining the gels at 550 °C do not contain nitrogen and the carbon content is less than 0.3%. A

(8) Bottero, J. Y.; Axelos, M.; Techoubar, D.; Cases, J. M.; Fripiat, J. J.; Fiessinger, F. *J. Colloid Interface Sci.* **1987**, *117*, 14.

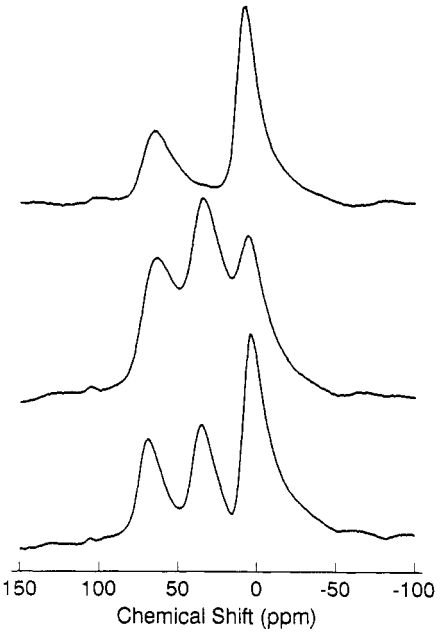

Figure 2. From bottom to top: (a) 111A gel; (b) 111 solid obtained upon calcination at 550 °C; (c) solid after calcination at 750 °C.

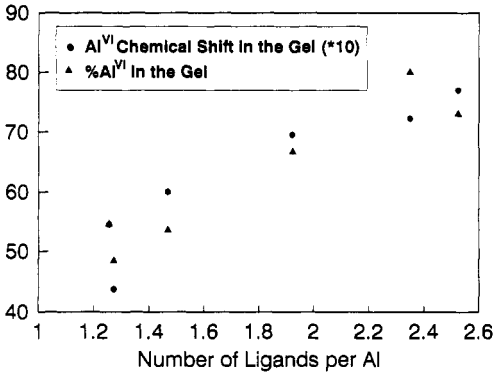

Figure 3. Either the $\%Al^{V}$ in the gel or 10 times the Al^{VI} line chemical shift in the gel *vs* the number of OH and *sec*-butoxyl ligands per Al (see Table I).

Table III. ^{27}Al MAS NMR Results Obtained for the Solid Calcined at 550 °C for 20 h. The Code Is the Same as in Table II (See Text for th.$\%Al^{V}_{(1)}$ and th.$\%Al^{V}_{(2)}$)

code	$\%Al^{IV}$	$\%Al^{V}$	$\%Al^{VI}$	th.$\%Al^{V}_{(1)}$	th.$\%Al^{V}_{(2)}$
111nW1	30.6	45.5	23.9	48.3	48.7
111 A	23.3	40.9	35.8	42.1	39.8
111	26.3	35.9	37.8	39.8	36.2
011	29.5	34.2	36.4	33.9	33.5
111W2	27.2	40.5	32.4	33.7	34.1
001	29.1	31.7	39.2	29.7	32
101	25.4	16.4	58.2	22.5	22
111NFD	30.9	17.8	51.3	20.5	19
112	24.9	19.3	55.8	16.9	19.1
012	22.5	15.3	62.1	15.3	13.3
00Ac	29.4	46.3	24.3	41.8	

typical ^{27}Al MAS NMR spectrum is shown in Figure 2b. Table III gives the Al^{IV}, Al^{V}, and Al^{VI} relative contents in the solids calcined for 20 h at 550 °C. After calcination at 750 °C, the Al^{V} line has almost disappeared (Figure 2c). It will be shown elsewhere that there are still a non-negligible content in Al^{V} in the subsurface layer.[9]

The first interesting observation in Table III is the quasi-constancy of the Al^{IV} content. In addition, the Al^{VI} line

(9) Coster, D.; d'Espinose, J. B.; Fripiat, J. J., manuscript in preparation.

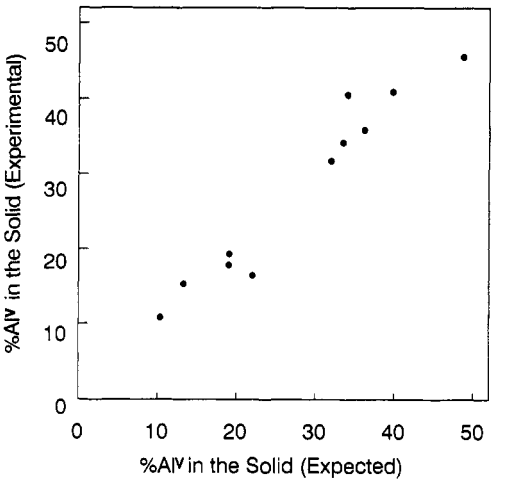

Figure 4. Structural memory: $\%Al^{V}$ in the solids *vs* (th.$\%Al^{V}_{(2)}$) obtained from eq 2.

chemical shifts are between 8 and 9 ppm. On the average, the Al^{IV} content is 27.2% ± 3.4%. In a spinel-like transition alumina the Al^{IV}/Al^{VI} ratio is 1/2. It is evident that the solids obtained here are far away from this composition. Since the Al^{IV} contents are approximately constant, the Al^{V} and Al^{VI} contents are inversely related. If one compares the characteristics of the gel (Table II) to the properties of the solids (Table III), it appears that the Al^{V} contents in the *solid* decreases as the degree of polymerization of the octahedral units in the *gel* increases. The Al^{V} content in the solid is linearly related to the Al^{VI} chemical shift of the gel by the following equation:

$$\%Al^{V} \text{ in the solid} = 73.2 - 7.33\ (Al^{VI} \text{ chemical shift in the gel, ppm}) \qquad R^2 = 0.897 \quad (1)$$

The $\%Al^{V}$ in the solid calculated from eq 1 is called the th.$\%Al^{V}_{(1)}$ in Table III. Taking into account the Al^{V} content of the gel improves the regression and it is observed that

$$\%Al^{V} \text{ in the solid} = 43.0 - 4.03\ (Al^{VI} \text{ chemical shift in the gel, ppm}) + 0.53\ (\%Al^{V} \text{ in the gel}) \qquad R^2 = 0.924 \quad (2)$$

The $\%Al^{V}$ in the solid calculated from eq 2 is th.$\%\ Al^{V}_{(2)}$ in Table III. Taking the percentage of Al^{V} in the gel into account improves the correlation coefficient. This is not surprising since the results in Table II show clearly that in the gels the Al^{V} content decreases as the Al^{VI} line shifts downfield. In Figure 4 the measured Al^{V} relative content in the solid is plotted against the theoretical Al^{V} content (th.$\%\ Al^{V}_{(2)}$) obtained from the eq 2. The slope is 1, and the intercept is 0.

The remarkable conclusion obtained from Figure 4 is that the solids keep the memory of the structural features of the gels. This is astonishing when one thinks about the deep structural rearrangement occurring during calcination. The *sec*-butoxyl residues burn producing CO_2 and H_2O and the residual water is removed. The solids calcined at 550 °C contain less than 1% water.

The Al^{V} species in the solids may be considered as coordinately unsaturated sites (CUS). In the gels where the Al^{V} and Al^{IV} contents are in the same order of magnitude (see Table II) it seems that a low average ratio ligands/Al favors the formation of the Al^{V} and Al^{IV} species which should be linked to scarcely polymerized Al^{VI}. In

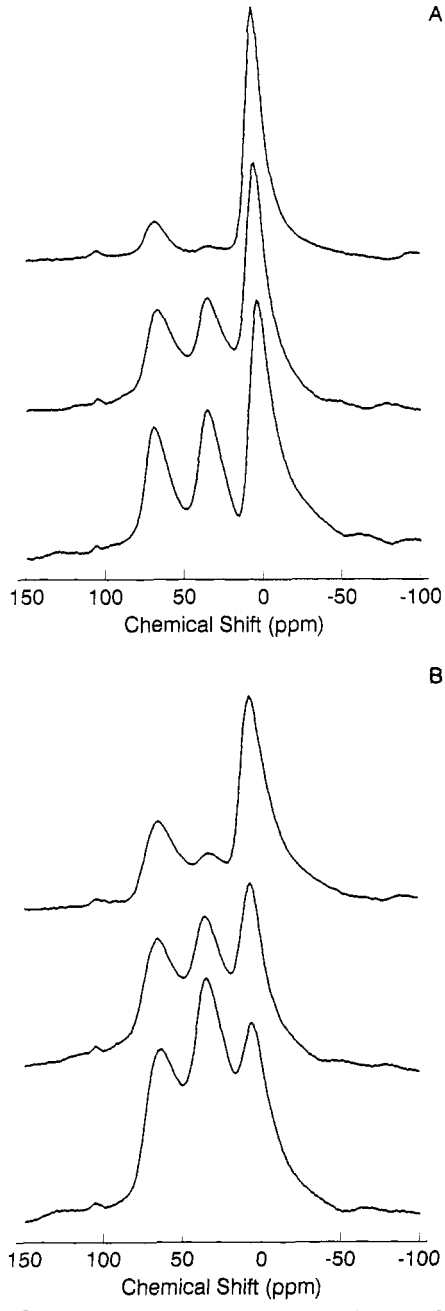

Figure 5. ^{27}Al MAS NMR spectra of gels: A (from bottom to top): 111A, 001 and 012. B: corresponding solids (calcination at 550 °C for 20 h).

spite of the fact that calcination increases the Al^{VI} condensation to its maximum, the structural rearrangement increases the Al^{V} contribution, while the Al^{IV} contents increase toward the value observed in pseudo-spinels.[2] The gel is transformed to the pseudo-spinel structure (Figure 1c) when calcined at a temperature higher than 700 °C, probably because of an increased mobility of the structural elements in the aluminum lattice. Figure 5 illustrates the structural relationship between gels and solids.

It is interesting at this point to examine an example of the TGA, DTG, and DTA diagrams shown in Figure 6. All the DTA traces obtained for eleven gels (see Table II) are similar. There is first an endothermic effect which has its maximum near 200 °C and a shoulder near 100 °C. It is followed by a high exothermic effect extending from 250 to 500 °C in which at least three contributions overlap.

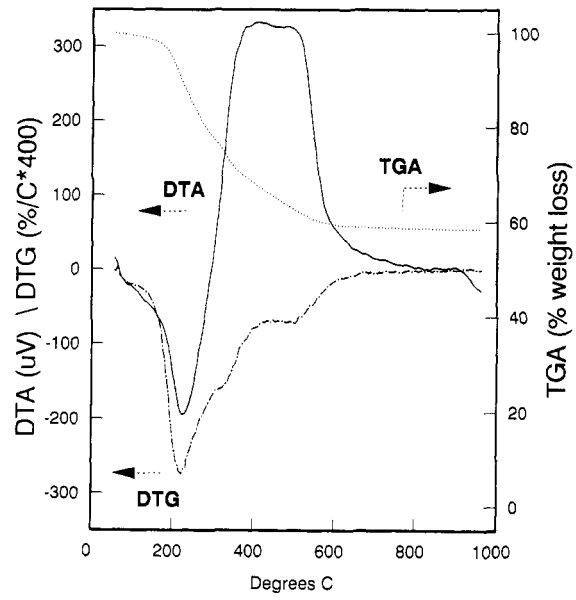

Figure 6. DTA, DTG, TGA diagrams of gel 111 (~200 mg of material). The DTG trace has been multiplied by 400.

The endothermic peak must correspond mainly to the removal of urea and to partial dehydroxylaion while the exothermic peak is due to the combustion of the *sec*-butoxyl residues. Urea melts at 135 °C and decomposes above 135 °C. Ammonium bicarbonate, which may be present in small amounts, melts at 107.5 °C and sublimates above that temperature. The boiling point of *sec*-butanol is 99.5 °C. These figures are taken from the CRC handbook.[10] Thus, if small amounts of urea, bicarbonate, and isobutanol remain in the gel, they may contribute to the exothermic effect and may be responsible for the shoulder observed near 100 °C. The DTG traces, which are the derivatives of the TGA (Figure 6), show consistently three main features: a deep minimum near 200 °C which corresponds to the minimum of the endothermic peak, a shoulder or a peak at ~300 °C and a second one near 500 °C. These shoulders or peaks correspond to the two contributions to the exothermic effect observed by DTA. They can be interpreted as follows: The *sec*-butoxyl residues are burned in two steps and an additional exothermic effect overlaps with the last step of the dehydroxylation process (*vide infra*). The ^{27}Al MAS NMR spectra observed in calcining the gels at increasing temperatures show that the Al^{V} relative content increases up to 450 °C and remains constant up to ~650 °C. Of course, these temperatures obtained for long time (20 h) calcinations cannot be compared with the features in TGA or DTA, since the latter are obtained for a dynamic process whereby the heating rate is 10 °C/min.

The metastability of the alumina rich in Al^{V} is demonstrated by the following experiments (see Figure 7). Solids 111 nW1 and 111 W2 were exposed for 24 h at 100% relative humidity at room temperature and the ^{27}Al MAS NMR spectra were recorded immediately after contact. Then the solids were recalcined at 550 °C. As shown in Table IV, the Al^{IV} contents did not change much, but the Al^{V} contents decreased very significantly. It

(10) *CRC Handbook of Chemistry and Physics*, 52nd ed.; The Chemical Rubber Co.: Cleveland, 1971–1972.

(11) The "3M" gels prepared by us were obtained from $Al(NO_3)_3$ and urea according to the procedure described in ref 3 and some minor modifications suggested by personal communication with Dr. Wood.

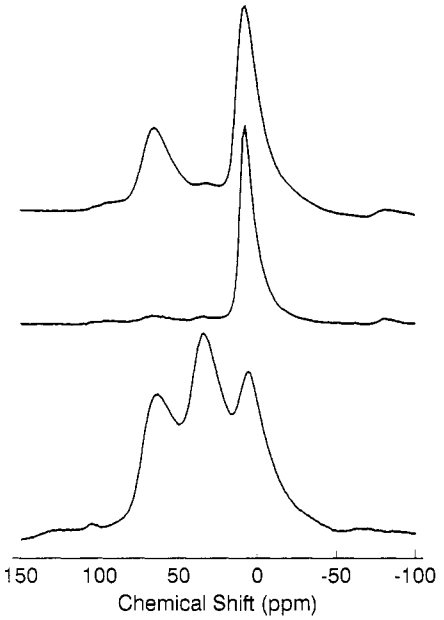

Figure 7. ^{27}Al MAS NMR spectra of (from bottom to top): 111W2 solid, the same exposed to saturated water vapor, and the hydrated solid recalcined for 20 h at 500 °C after rehydration.

Table IV. ^{27}Al MAS NMR Results Obtained for the Solids before Rehydration or after Rehydration and Recalcination at 550 °C for 20 h

code	$\%Al^{IV}$	$\%Al^{V}$	$\%Al^{VI}$
111nW1	30.6	45.5	23.9
111nW1r	24.4	28.2	47.9
111W2	27.2	40.5	32.4
111W2r[a]	29.1	10.8	60

[a] r means rehydrated.

Table V. Textural Characteristics of the Solids: Pv < 6 nm: Cumulative Pore Volume (mL/g) in Pores with Diameters < 6 nm; %Pv < 6 nm: Volume Percent of These Pores. A: BET Surface Area (N_2, −196 °C)

code	Pv < 6 nm	%Pv < 6 nm	A ($m^2\ g^{-1}$)
111A	0.401	91	278
111	0.36	86	287
00Ac	0.112	82	202
011	0.401	69	330
111W2	0.759	59	301
001	0.617	53	273
112	0.916	44	343
101	0.84	30	258
111NFD	0.713	40	288

decreases further after a second cycle of rehydration and calcination (not shown). Thus, rehydration and recalcination eliminate progressively the CUS. How easily a solid calcined at 550 °C for 20 h readsorbs water was unexpected. The ^{27}Al MAS NMR spectra taken on solids exposed to the atmosphere for more than 1 week did not change appreciably with respect to those recorded after calcination and storage over P_2O_5.

B. Textural Aspects. From the N_2 adsorption–desorption isotherms, the BET surface area, and the pore volume (Pv) distribution are computed, see Table V. The pore-size distributions $\delta Pv/Pv\delta d$ exhibit a narrow peak for pore diameters (d) between 4 and 5.5 nm. The amplitude of this maxima decreases with decreasing Al^V contents in the solids (see Figure 8 and Table III). Since the relative concentration of Al^V (CUS) sites in the bulk is related to the pore distribution, there should be a correlation between the percent of small pores ($d < 6$ nm)

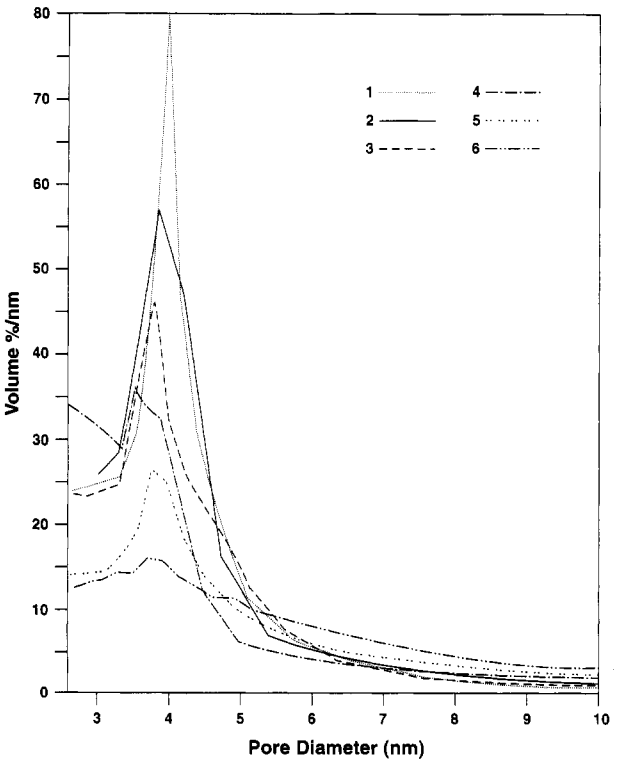

Figure 8. Relative pore-size distribution $(1/P_v)(\delta P_v/\delta d)$ with respect to the diameter d (nm) in six solids obtained from gels: (1) 111A (41%); (2) 00Ac (46.3%); (3) 011 (34.2%); (4) 012 (15.3%); (5) 001 (31.7%); (6) 112 (19.3%). The number is parentheses corresponds to the relative Al^V content.

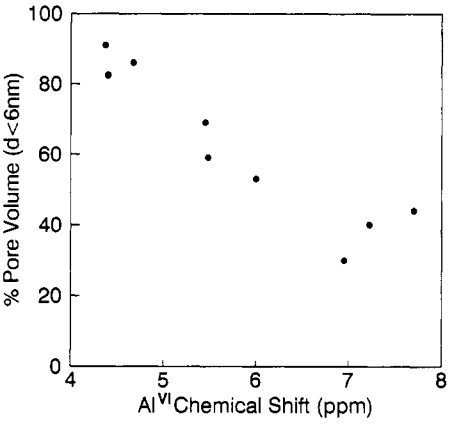

Figure 9. Textural memory: percent cumulative pore volume in pores with diameter smaller than 6 nm in the solid *vs* the degree of condensation of the Al octahedra in the gel.

in the *solids* and the degree of polymerization of the octahedra in the *gels*.

The percent cumulative pore volumes in pores with a diameter smaller than 6 nm (%Pv < 6 nm) are given in Table V, while the correlation with the Al^{VI} line chemical shift in the corresponding gel is obvious in Figure 9. This correlation indicates that the texture of the solid keeps in memory the degree of condensation of the octahedra in the gel. Thus, in addition to the structural memory displayed in Figure 4, there is a textural memory (Figure 9). Maybe the existence of a narrow pore distribution in the 111 solids and the relationship between the distribution and the Al^V content explains the metastability reported in Table V. By capillary condensation at 100% relative humidity these pores are filled with water, and in addition crevices not available to N_2 are available to water. The

chemical driving force corresponding to the $Al^V + H_2O \rightarrow Al^{VI}$ reaction may be large enough to allow H_2O to diffuse towards surfaces unavailable to N_2, such as internal surfaces at grain boundaries where CUS may be concentrated. This hypothesis is supported by the fact that there is apparently no correlation between the relative Al^V content and the surface area of the solid (Tables III and V), measured with N_2.

Discussion and Conclusion

The initial motivation of this contribution was to demonstrate the memory effect in gel–solid transformation. The preparation procedure has been varied to obtain non-equivalent gels. It has been observed (Figures 4 and 5) that the evolution of the gel upon thermal activation is determined by its initial structure. The chemical shift of the Al^{VI} and the Al^V content are the important information characterizing the gel and they enable one to predict the thermal evolution. The notion of *structural* memory is based on this observation. *Textural* memory effects have also been evidenced (Figures 8 and 9), i.e., the pore size distribution and the total volume of small pores are related to the extent of polymerization monitored by the Al^{VI} chemical shift in the gel. These effects are not trivial considering (i) the severity of the thermal treatment, the extent of the weight loss and the intensity of the endo- and exothermic effects (Figure 6) during calcination, and (ii) the modifications of the preparation procedure and the difficulty to control all the factors involved. For instance, the freeze-drying step is difficult to master. Its efficiency is affected by the residual amount of *sec*-butanol left after centrifugation. Moreover, the drying process has been carried out at temperatures between 70 and 85 °C.

The specific role of the different additives are not always easy to evidence, but the following conclusions can be drawn: the partial hydrolysis induced by the limited amount of water present in the system is the most critical parameter. When the water content increases, the polymerization is enhanced. The effect of ammonium bicarbonate is evident. In spite of its poor solubility in *sec*-butanol, it induces the flocculation of the gel. The role of urea is not clear. It seems to prevent the octahedral condensation (compare Al^{VI} shift for 111A or 111 and 011 in Table II), but the comparison of gels 101 and 011 shows a reverse tendency. To what extent the large amount of water produced above 300 °C in the combustion of the *sec*-butoxyl residues is important in the structural rearrangement is an open question.

As already mentioned before, the "3M process" described by Wood *et al.*[6] also leads to Al^V rich solids. Gels and solids produced by both synthesis pathways have been compared.[11] From the DTA point of view, the results are very different. Of course, the 3M gel does not show the large exothermic effect between 300 and 500 °C. Moreover, an endo- and exothermic peak is observed near 300 and 900 °C, respectively. The last one is barely observed in our DTA diagrams. In both cases, the DTG is mainly characterized by a minimum near 200 °C. The sharp minimum near 400–410 °C observed for the 3M gel might correspond to the shallow features that we record between 400 and 500 °C. From the ^{27}Al NMR point of view, it is important to mention that the Al^{VI} line shift for the 3M gels is always between 8 and 9 ppm. No structural memory can be evidenced. The surface areas of the 3M solid (gels calcined at 550 °C for 20 h) were always between ~100 and ~160 $m^2\ g^{-1}$, that is appreciably smaller than those reported in Table V. The pore-size distribution of the 3M solids did not show the well-pronounced maxima exhibited by our solids (Figure 8). These differences are concurrent with the fact that in the water the degree of condensation of the octahedral units is high.

The numerous differences between samples produced by the two methods raise one inevitable question. Why do they lead to similar unusual aluminas? The 3M gels are prepared in aqueous solution whereas an excess of water poisoned the formation of Al^V in the alkoxide route. Moreover, urea does not play a central role in our procedure as it does in the 3M gel preparation. Nevertheless, the similarity between the solids could be traced to what is happening in the sol. In both cases, small Al oligomers are produced because either urea stop the crystal growth (3M) or the limited amount of water prevents extensive polymerization in the alkoxide procedure. During precipitation and drying, the small oligomers agglomerate into larger particles. At the intergranular border, the number of CUS is high and the pentacoordinated aluminum is revealed by the calcination. A similar picture could be drawn for the grinding process. Hence, the intergranular surface (only partially accessible to N_2) seems to be the important factor related to the Al^V content.

To what extent a similar explanation could be extended to the solids rich in Al^V described by Nazar *et al.*[12] in unknown. These authors have observed that the sulfate of an Al_{13} polyoxycation dimer, calcined at increasing temperature, undergoes a deep structural rearrangement. Below 200 °C, the ^{27}Al NMR features are similar to those described for Al_{13},[8] namely, resonances corresponding to Al^{IV} and Al^{VI}. Above 500 °C, the ^{27}Al MAS NMR spectrum is similar to that shown in Figure 2b. The role of the sulfate is not known. We have observed a similar behavior in calcining an aluminum acetate obtained by precitation from an $Al(NO_3)_2$ solution, except that the starting acetate contained Al^{VI} only.

Acknowledgment. This work has been made possible by DOE Grant DOE-FG02-90ER1430. Discussions with T. E. Wood are deeply acknowledged. We thank Dr. J. M. Dominguez of the Mexican Institute of Petroleum (Materials and Catalysis Division) for the TEM picture.

(12) Nazar, L. F.; Fu, G.; Bain, A. D. *J. Chem. Soc., Chem. Commun.* **1992**, 251.